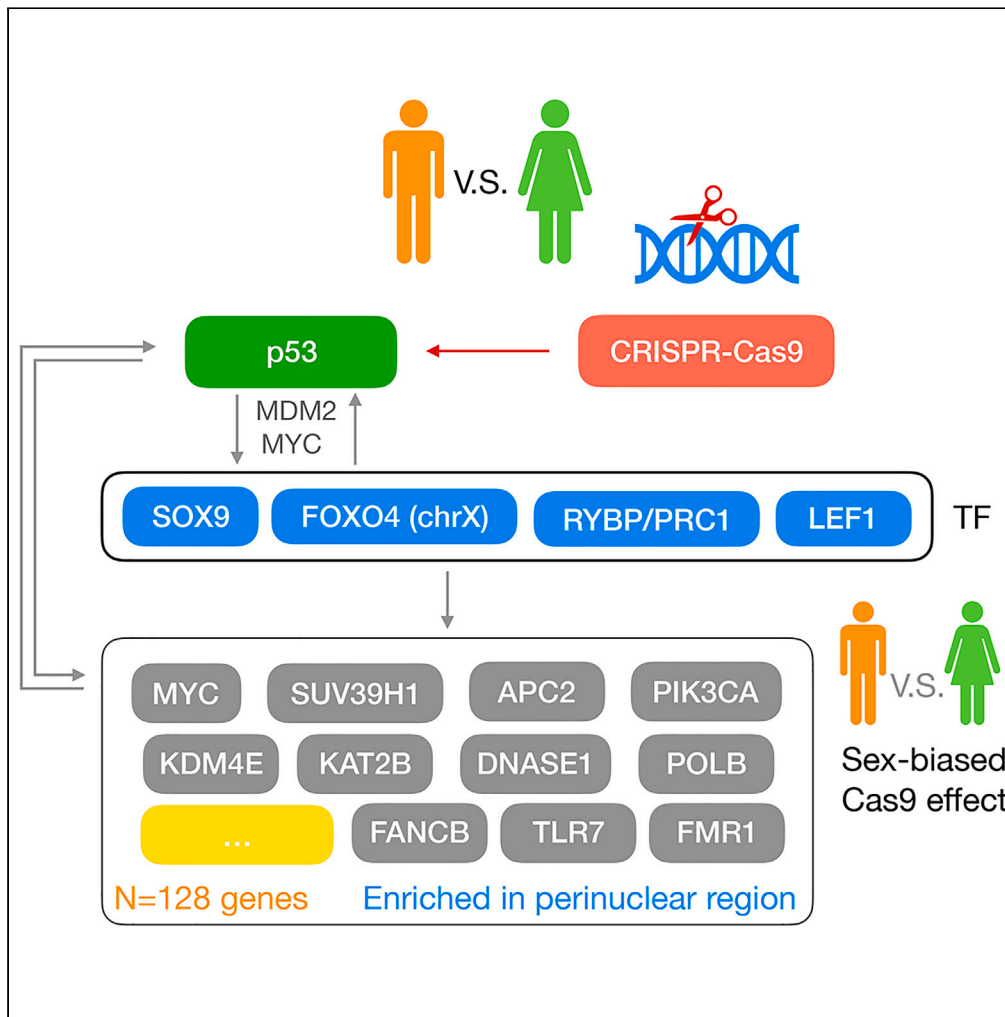


Article

Sex-biased genome-editing effects of CRISPR-Cas9 across cancer cells dependent on p53 status



Mengbiao Guo,
Yuanyan Xiong

guomengbiao@gmail.com (M.G.)
xyyan@mail.sysu.edu.cn (Y.X.)

Highlights

Large sex-biased difference of Cas9 activities between cell lines with wildtype and mutant p53

>100 genes (including MYC and PIK3CA) showed knockout sex bias in CRISPR-Cas9 screens

Four TFs (SOX9, FOXO4, LEF1, and RYBP) responsible for sex bias effects of CRISPR-Cas9



Article

Sex-biased genome-editing effects of CRISPR-Cas9 across cancer cells dependent on p53 status

Mengbiao Guo^{1,*} and Yuanyan Xiong^{1,2,*}

SUMMARY

The CRISPR-Cas9 system has emerged as the dominant technology for gene editing and clinical applications. One major concern is its off-target effect after the introduction of exogenous CRISPR-Cas9 into cells. Several previous studies have investigated either Cas9 alone or CRISPR-Cas9 interactions with p53. Here, we reanalyzed previously reported data of p53-associated Cas9 activities and observed large significant sex differences between p53-wildtype and p53-mutant cells. To expand the impact of this finding, we further examined all protein-coding genes for sex-specific dependencies in a large-scale CRISPR-Cas9 screening dataset from the DepMap project. We highlighted the p53-dependent sex bias of gene knockouts (including *MYC*, *PIK3CA*, *KAT2B*, *KDM4E*, *SUV39H1*, *FANCB*, *TLR7*, and *APC2*) across cancer types and potential mechanisms (mediated by transcriptional factors, including *SOX9*, *FOXO4*, *LEF1*, and *RYBP*) underlying this phenomenon. Our results suggest that the p53-dependent sex bias may need to be considered in future clinical applications of CRISPR-Cas9, especially in cancer.

INTRODUCTION

CRISPR-Cas9, an emerging powerful genome-editing system originated from bacteria, is known to interact with p53.^{1–5} This system can inactivate genes in a precise manner, relying on DNA breaks and repair, which are mostly guarded by p53. Enache et al.⁶ have recently demonstrated that the protein Cas9 alone can activate the p53 pathway and select for p53-inactivated mutants. Briefly, they investigated the effects of Cas9 introduction on cells at the mRNA and protein levels, especially for the p53 pathway, and they further studied the differential Cas9 activities in cell lines with a wildtype (WT) or mutant (MUT) p53. They found that Cas9 introduction will activate the p53 pathway and select p53-inactivating mutations in examined cell lines. However, the potential sex bias of Cas9 introduction has not been considered yet. p53 is differentially regulated in both healthy and cancer samples between females and males.⁷ Our recent work also shows that p53 regulates the active X chromosome dosage compensation, but with different effect sizes between sexes.⁸ Importantly, some vital genomic regulators interacting with p53 are encoded by genes on chromosome X, which contributed to the sex bias of p53 activity, especially in cancer.⁷ Here, we evaluated the potential sex bias of both Cas9 alone and CRISPR-Cas9 across cell types systematically.

RESULTS

We found that the largest effects of many results shown by Enache et al. were from cell lines from female donors, including the largest fold-change of p53 activation (BT159: female), more DNA damage foci (MCF7: female), and the largest TP53-inactivating subclonal mutations expanding or shrinking (293T, HCC1419, and OVK18: female, Figure 1A). In contrast, the difference of Cas9 activity between p53-WT (wildtype) and p53-MUT (mutant) cells was larger in male (two-sided t-test, $p = 3.1E-5$, difference 14.85%) than female lines (two-sided Wilcoxon-test, $p = 0.021$, difference 7.46%). The difference was much larger (p -value $< 2e-16$, see STAR Methods) in male compared with female cell lines (Figures 1B and 1C). These observations clearly demonstrated significant sex bias of Cas9 functions in mammalian cells. These results possibly reflect the sex-biased effects of Cas9 due to the differential functions and regulations of p53 between sexes.

¹Key Laboratory of Gene Engineering of the Ministry of Education, Institute of Healthy Aging Research, School of Life Sciences, Sun Yat-sen University, Guangzhou 510006, China

²Lead contact

*Correspondence: guomengbiao@gmail.com (M.G.), xyyan@mail.sysu.edu.cn (Y.X.)
<https://doi.org/10.1016/j.isci.2023.107529>



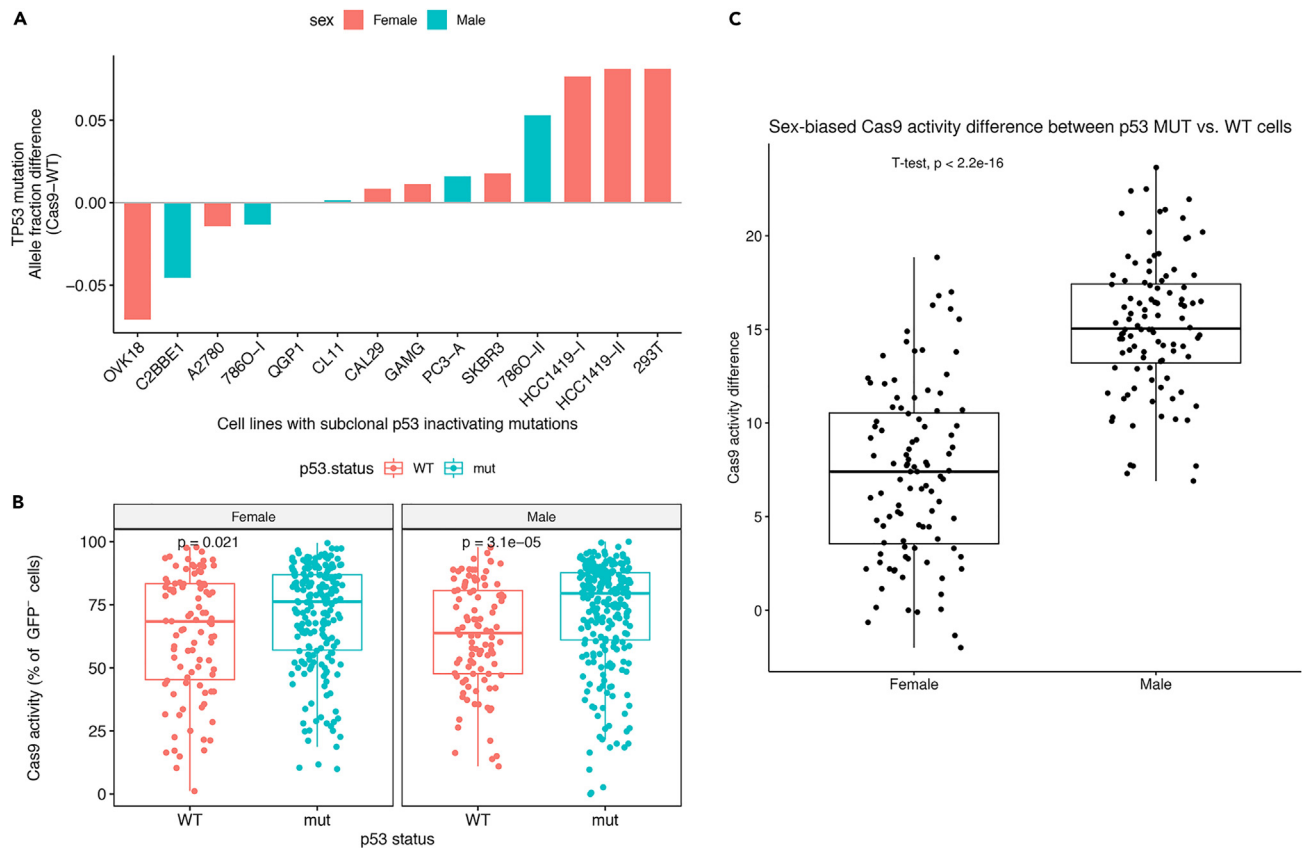


Figure 1. Sex-biased activities of Cas9 across cell lines are dependent on p53 status

(A) TP53 allele fraction differences (y axis) after Cas9 introduction in various cell lines (x axis), colored by sexes.

(B) Comparison of Cas9 activities (y axis) between p53-WT and p53-MUT (x axis) in male cell lines (right) and in female cell lines (left).

(C) Boxplots showing sex-biased (x axis) Cas9 activity difference (y axis) between p53-WT and p53-MUT cell lines shown in (B). (B and C) Data are represented as median \pm IQR in boxplots (bar, median; box, 25th and 75th percentile; whiskers, 1.5 times the interquartile range (IQR) of the lower and upper quartiles; points, individual cell lines). Two-sided Wilcoxon-test.

Due to the potentially large-scale clinical usage of CRISPR-Cas9 in the future in patients with various diseases, sex-specific effects should be studied carefully and considered beforehand. However, we have found no report discussing sex-biased CRISPR-Cas9 knockout (KO) effects to date. We thus investigated the potential p53 status-dependent sex bias in the CRISPR screening data from the DepMap⁹ project (22Q4, <https://depmap.org/portal/>). Our rationale is that if the CRISPR-Cas9 KO effect of a gene shows significant sex bias and is p53 status-dependent, two scenarios may occur: (1) this sex difference can only be detected within either p53-WT or p53-MUT cell lines; (2) the sex difference can be detected in both p53-WT and p53-MUT cell lines but their magnitudes differ significantly. This study only aimed to propose the concept of p53 status-dependent sex bias in CRISPR-Cas9 editing and provide basic evidence; therefore, the second scenario was not considered here because it was more complex, although we believe it may provide more significant genes and thus more insight.

First, we obtained a list of 65 genes showing significant p53-dependent sex-bias of KO effects (defined by the depletion of guide RNAs [gRNA] after CRISPR-Cas9 introduction into cells) by comparing CRISPR-Cas9 editing effect scores (calculated by the DepMap project) on genes between cell lines from male and female donors for each tissue (Tables 1 and S1). Examples include DNASE1 (Deoxyribonuclease 1, female-biased), POLB (DNA Polymerase Beta, male-biased), DFFA (DNA Fragmentation Factor Subunit Alpha, male-biased), FANCB (Fanconi Anemia Group B Protein involved in DNA repair, female-biased), APC2 (Adenomatous Polyposis Coli 2, female-biased), KAT2B (Histone Acetyltransferase PCAF, female-biased), and KDM4E (Lysine (K)-Specific Demethylase 4E, male-biased) (Figures 2A–2G). Eight of these 65 genes were only identified by using genes (gene set 1, with less burden of multiple testing correction) whose products

Table 1. PCSB genes that show significantly sex-biased effects in CRISPR-Cas9 screening experiments

p53 status	Gene set	Sex bias	Significant genes
WT	PPI-p53	M	<i>ILK, PSMC4, RANBP2</i>
		F	<i>AIFM1, CAPN6, EDA2R, FGF13, MYC, PIK3CA, PPEF1, SUV39H1, TLR7</i>
	All	M	<i>C17orf80, CCDC71, CCK, CCNL1, CLCN1, CLDN19, CNPY3, CYP3A4, DCP1B, GPN2, JADE2, KDM4E, MOGAT3, MYL3, NCK2, NFKBIL1, OSTN, PELI2, PHTF1, POLB, PTPA, SDC1, SIT1, SPRYD7, STRN4, TMEM178B, UGT1A5, ZNF138</i>
MUT	PPI-p53	M	<i>BAZ2B, DFFA, DUSP26, FEN1, PRKRA</i>
		F	<i>DNASE1, KAT2B</i>
	All	M	<i>CFHR3, ECRG4, MEX3D, RHD</i>
		F	<i>APC2, H2AC16, MID2, NACA2, SLC6A14</i>

M: Male, F: Female.

with p53 protein-protein interactions (PPI, from the STRING database <https://string-db.org/>, see [STAR Methods](#) for details), but not by using all protein-coding genes (gene set 2). Only eight of the 65 genes were located on the X chromosome. Moreover, only 13 of the 65 genes were significant in p53-MUT samples, including H2AC16 (HIST1H2AL, H2A Clustered Histone 16, female-biased), APC2, DFFA, DNASE1, PRKRA (Protein Activator Of Interferon Induced Protein Kinase EIF2AK2/PKR, male-biased), KAT2B, FEN1 (Flap Structure-Specific Endonuclease 1, male-biased). Moreover, we found sex-biased KO effects in both p53-WT and p53-MUT cells, but not for *TP53* (however, note that its negative regulator *MDM2* had a suggestive p-value of 0.0016 (two-sided t-test; male-biased) only in brain cells, which may help explain the p53 activation results in brain tumor BT159.⁶ Of note, the *FANCB* of the Fanconi Anemia (FA) pathway has been identified to play a key role in CRISPR-Cas9 editing.¹⁰

Moreover, we conducted a cross-tissue investigation of sex-biased gene editing effects after controlling for tissue types, which resulted in another 64 significant genes (CNGA2 [Cyclic Nucleotide Gated Channel Subunit Alpha 2] was also identified in single-tissue analysis above, female-biased), such as *MYC* (Myc Proto-Oncogene Protein, female-biased), *SUV39H1* (*SUV39H1* Histone Lysine Methyltransferase, also known as *KMT1A*, female-biased), *FMR1* (Fragile X Messenger Ribonucleoprotein 1, female-biased), *PIK3CA* (PtdIns-3-Kinase Catalytic Subunit Alpha, female-biased), and *TLR7* (Toll Like Receptor 7, female-biased) (Figures 2H–2K; Tables 1 and S1). Notably, only 3 out of 64 genes, *MID2* (Midline 2, RING-Type E3 Ubiquitin Transferase), *CFHR3* (Complement Factor H Related 3), and *SLC6A14* (Solute Carrier Family 6 Member 14), were identified as significant in p53-MUT samples (Figure 2K, note that *DDX3X*, *EIF1AX*, *RPS4X*, *ZFX*, *MAGEH1*, and *VBP1* were excluded because they were identified as significant in both p53-WT and p53-MUT samples), consistent with the single-tissue analysis results above. In contrast to single-tissue analysis, 52 out of 64 genes were located on chromosome X (Table S1). Interestingly, p53 can regulate *MYC* in various ways and vice versa.^{11–18} The function of *MYC* was controlled by the androgen receptor (AR)/p53 axis,¹⁸ and by *DDX3Y* in male of *MYC*-driven lymphomas with *DDX3X*-inactivation.¹⁹ Additionally, *MYC* is a direct target of *APC* (WNT Signaling Pathway Regulator), the paralog of *APC2* from the 64 genes.²⁰

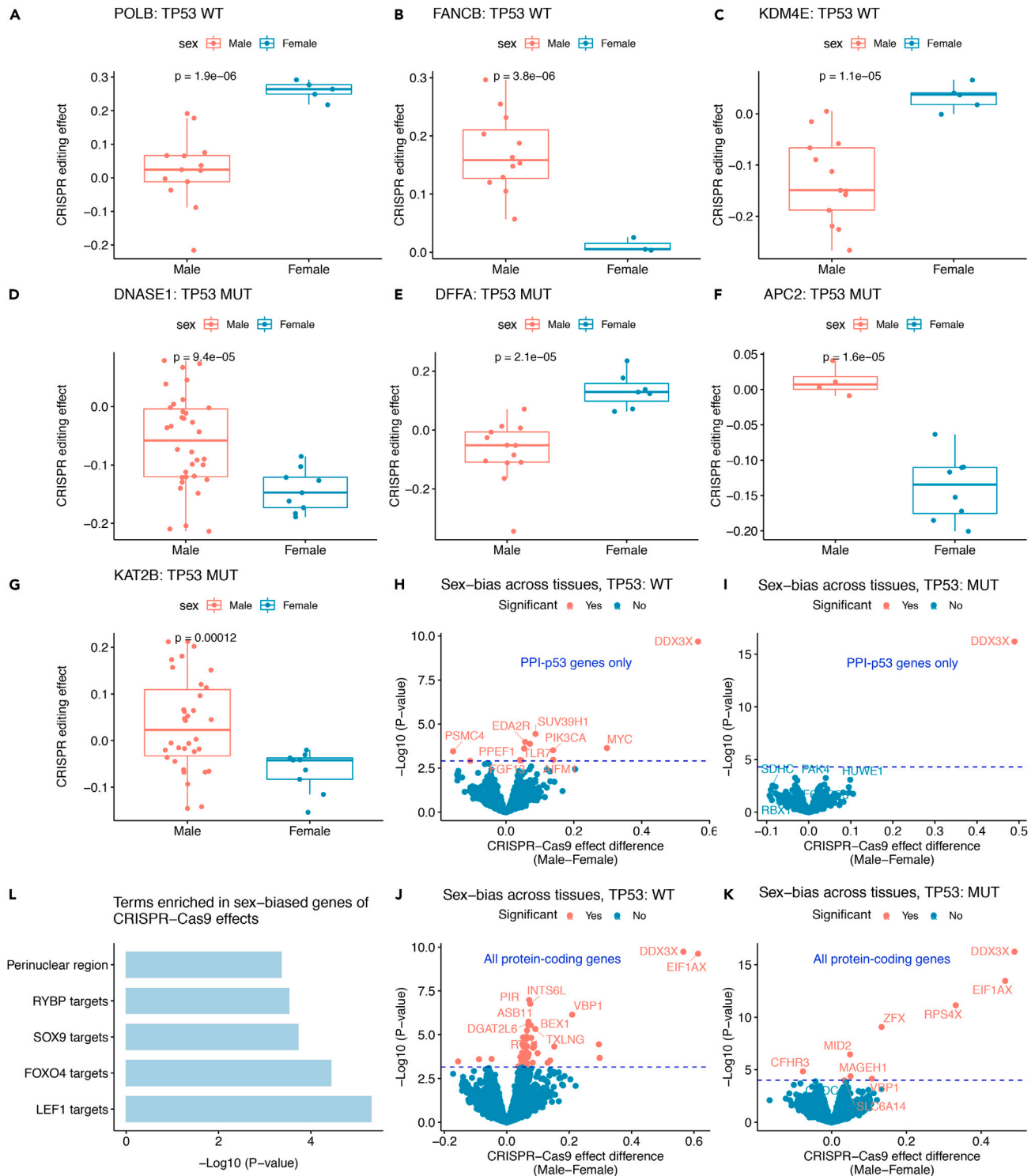


Figure 2. Sex-biased gene editing effects by CRISPR-Cas9 in cancer cells are dependent on p53 status

(A–G) Boxplots showing PCSB genes with sex-biased KO effects in CRISPR-Cas9 screening in a specific cancer cell type with (TP53-MUT) or without (TP53-WT) p53-inactivating mutation. Dots represent samples and were colored by sex. Two-sided t-test. Data are represented median \pm IQR in boxplots (bar, median; box, 25th and 75th percentile; whiskers, 1.5 times the IQR of the lower and upper quartiles; points, individual cell lines). Two-sided Wilcoxon-test. (H–K) Volcano plots showing significantly sex-biased CRISPR-Cas9 KO effects (y axis: p-values, x axis: gene editing effect differences) across cancer types with TP53-MUT (H, J) or TP53-WT (I, K), based on genes encoding proteins interacting with p53 only or all protein-coding genes. The ten most promising

Figure 2. Continued

genes to show sex bias, ranked by nominal p-values, were labeled. Dashed blue lines represent significance cutoff after multiple testing correction by false discovery rate (FDR).

(L) Barplots showing the significance of enrichment in targets of four transcription factors (TFs, including RYBP, SOX9, FOXO4, and LEF1) or in perinuclear regions for p53-dependent sex-biased genes of CRISPR-Cas9 editing.

To further reveal the potential mechanism of p53 regulating Cas9 activities in human cells, we performed functional enrichment analysis for all these 128 significant genes with p53-dependent CRISPR-Cas9 sex bias (termed PCSB genes). We observed that they were enriched in perinuclear regions ($p = 5.0e-6$, reported by the webserver of ToppGene,²¹ <https://toppgene.cchmc.org/enrichment.jsp>) and in target genes of four transcription factors (TF): LEF1 ($p = 3.7e-5$, reported by the webserver of ToppGene; Lymphoid Enhancer Binding Factor 1), FOXO4 ($p = 1.9e-4$; Forkhead Box O4), SOX9 ($p = 3.0e-4$; SRY-Box Transcription Factor 9), and RYBP ($p = 4.4e-4$; RING1 And YY1 Binding Protein) (Figure 2L). We believe these TFs are potential drivers of the sex bias studied in this work.

Three of the four TFs were directly linked to sex or sex chromosomes. First, the gene encoding FOXO4 is located on chromosome X. FOXO4 has PPI interaction with p53^{22,23} and also MDM2 (Mouse Double Minute 2), the prime E3 ligase for p53.^{24,25} Moreover, PIK3CA is the catalytic subunit of PI3K and FOXO4 is a downstream effector of the PI3K/AKT pathway.²⁶ Second, RYBP is a component of the Polycomb group (PcG) protein complex 1 (PRC1) that mediates the histone modification of H2AK119ub and is required for X chromosome inactivation (XCI) in females.²⁷ RYBP can stabilize p53 by modulating MDM2.²⁸ Third, SOX9 on chromosome 17 is a direct target of SRY (Sex-Determining Region Y) and, together with its distal enhancer, is critical in mammalian sex determination.²⁹ SOX9 can regulate MYC expression by interacting with FOXO1.³⁰ The remaining TF, LEF1, can be induced by MYC to activate the WNT pathway and sustain cell proliferation.³¹ LEF1 can also activate MYC or CCND1 to enhance pancreatic tumor cell proliferation.^{32,33}

Of note, p53 can negatively regulate SUV39H1 to remodel H3K9me3-marked constitutive heterochromatin by recruiting HP1,^{34,35} while SUV39H1 is functionally linked with PRC1.³⁶ MYC is also an important interactor with another PRC1 subunit YAF2 (YY1 Associated Factor 2).³⁷ Consistently, a recent study reported higher activity of CRISPR-Cas9 in active chromatin than in heterochromatin regions,³⁸ therefore, it is possible that p53-dependent sex-biased CRISPR-Cas9 activity was mediated by chromatin remodelers, such as PRC1, SUV39H1, KAT2B, and KDM4E.

Finally, a recent report reported both CRISPR-specific differentially essential positive (CDE+) and CDE- genes dependent on TP53 or KRAS.³⁹ We found that PCSB genes were in both TP53-dependent CDE+ genes (CCNL1, FAM210A, MOGAT3, and FKBPL) and CDE- genes (NEUROD4), and in KRAS-dependent CDE- genes (PELI2, NACA2, and RMI1) reported by Sinha et al.³⁹ More importantly, we have detected sex bias in genes of potential CRISPR-selected cancer drivers (CCD) similar to TP53 from the same study.³⁹ These genes include PIK3CA (FDR = 3.2e-29 as reported by Sinha et al.) and the paralog of APC2 (APC, FDR = 0.1) from our PCSB genes. Interestingly, SOX9 (FDR = 2.5e-9 as reported by Sinha et al., one of the four TFs with targets enriched in our PCSB genes) was also among their CCD genes.

DISCUSSIONS

We summarized our findings and proposed potential mechanisms that p53 can affect CRISPR-Cas9 effects in mammalian cells (Figure 3). Collectively, our work demonstrates the potential sex-biased gene editing effects both at the genome-wide level based on Cas9 itself and for specific genes based on CRISPR-Cas9 screening results. We suggest that the sex bias effect may need to be considered in future clinical applications (e.g., targeting MYC, PIK3CA, APC2, FANCB, KAT2B, KDM4E, TLR7, and SUV39H1 from our PCSB genes), especially in cancer, when using CRISPR-Cas9 and potentially other Cas protein systems.

Limitations of the study

Although this analysis presents many interesting new findings based on large-scale screening datasets of Cas9 alone or the CRISPR-Cas9 system, we did not perform experimental work to support our findings. Moreover, we note considerable difference between analysis results based on two recent versions of DepMap, 20Q4 and 22Q2, which may reflect both the impact of dramatic expanding the number of cell

Working Model

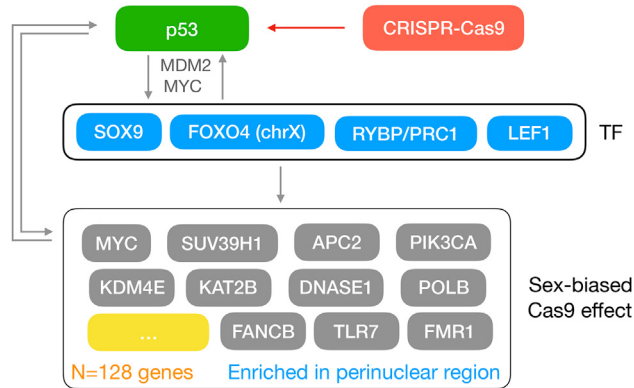


Figure 3. The proposed working model showing potential mechanisms p53 status can affect CRISPR-Cas9 editing effects differently between sexes in mammalian cells

p53 may affect CRISPR-Cas9 in a sex-dependent way either directly by regulating some of the sex-biased genes or indirectly by regulating four TFs, SOX9, FOXO4, RYBP, or LEF1, which may in turn be mediated by MDM2 or MYC.

lines and the large heterogeneity of cell lines within each lineage, and therefore, experimental follow-up work is needed.

STAR★METHODS

Detailed methods are provided in the online version of this paper and include the following:

- KEY RESOURCES TABLE
- RESOURCE AVAILABILITY
 - Lead contact
 - Materials availability
 - Data and code availability
- METHOD DETAILS
 - Data collection, preprocessing, and summary
 - Enrichment analysis
- QUANTIFICATION AND STATISTICAL ANALYSIS

SUPPLEMENTAL INFORMATION

Supplemental information can be found online at <https://doi.org/10.1016/j.isci.2023.107529>.

ACKNOWLEDGMENTS

We thank the DepMap and CCLE projects for making their datasets available for analysis. The research has been supported by Integrated Project of Major Research Plan of National Natural Science Foundation of China (NSFC) (92249303), Guangdong Basic and Applied Basic Research Foundation (2021A1515110972), and Fundamental Research Funds for the Central Universities - Sun Yat-sen University (23ptpy62).

AUTHOR CONTRIBUTIONS

M.B.G. conceived the idea, performed the analysis, and drafted the manuscript. Y.Y.X. provided writing input. Both authors reviewed the manuscript.

DECLARATION OF INTERESTS

The authors declare no competing interests.

INCLUSION AND DIVERSITY

We support inclusive, diverse, and equitable conduct of research.

Received: November 14, 2022

Revised: June 12, 2023

Accepted: July 28, 2023

Published: August 3, 2023

REFERENCES

- Ihry, R.J., Worringer, K.A., Salick, M.R., Frias, E., Ho, D., Theriault, K., Kommineni, S., Chen, J., Sondey, M., Ye, C., et al. (2018). p53 inhibits CRISPR-Cas9 engineering in human pluripotent stem cells. *Nat. Med.* 24, 939–946. <https://doi.org/10.1038/s41591-018-0050-6>.
- Haapaniemi, E., Botla, S., Persson, J., Schmierer, B., and Taipale, J. (2018). CRISPR-Cas9 genome editing induces a p53-mediated DNA damage response. *Nat. Med.* 24, 927–930. <https://doi.org/10.1038/s41591-018-0049-z>.
- Wu, Y., Zeng, J., Roscoe, B.P., Liu, P., Yao, Q., Lazzarotto, C.R., Clement, K., Cole, M.A., Luk, K., Baricordi, C., et al. (2019). Highly efficient therapeutic gene editing of human hematopoietic stem cells. *Nat. Med.* 25, 776–783. <https://doi.org/10.1038/s41591-019-0401-y>.
- Schirotti, G., Conti, A., Ferrari, S., Della Volpe, L., Jacob, A., Albano, L., Beretta, S., Calabria, A., Vavassori, V., Gasparini, P., et al. (2019). Precise Gene Editing Preserves Hematopoietic Stem Cell Function following Transient p53-Mediated DNA Damage Response. *Cell Stem Cell* 24, 551–565.e8. <https://doi.org/10.1016/j.stem.2019.02.019>.
- Brown, K.R., Mair, B., Soste, M., and Moffat, J. (2019). CRISPR screens are feasible in TP53 wild-type cells. *Mol. Syst. Biol.* 15, e8679. <https://doi.org/10.15252/msb.20188679>.
- Enache, O.M., Rendo, V., Abdusamad, M., Lam, D., Davison, D., Pal, S., Currimjee, N., Hess, J., Pantel, S., Nag, A., et al. (2020). Cas9 activates the p53 pathway and selects for p53-inactivating mutations. *Nat. Genet.* 52, 662–668. <https://doi.org/10.1038/s41588-020-0623-4>.
- Haupt, S., Caramia, F., Herschtal, A., Soussi, T., Lozano, G., Chen, H., Liang, H., Speed, T.P., and Haupt, Y. (2019). Identification of cancer sex-disparity in the functional integrity of p53 and its X chromosome network. *Nat. Commun.* 10, 5385. <https://doi.org/10.1038/s41467-019-13266-3>.
- Guo, M., Fang, Z., Chen, B., Songyang, Z., and Xiong, Y. (2023). Distinct dosage compensations of ploidy-sensitive and -insensitive X chromosome genes during development and in diseases. *iScience* 26, 105997. <https://doi.org/10.1016/j.isci.2023.105997>.
- Meyers, R.M., Bryan, J.G., McFarland, J.M., Weir, B.A., Sizemore, A.E., Xu, H., Dharia, N.V., Montgomery, P.G., Cowley, G.S., Pantel, S., et al. (2017). Computational correction of copy number effect improves specificity of CRISPR-Cas9 essentiality screens in cancer cells. *Nat. Genet.* 49, 1779–1784. <https://doi.org/10.1038/ng.3984>.
- Richardson, C.D., Kazane, K.R., Feng, S.J., Zelin, E., Bray, N.L., Schäfer, A.J., Floor, S.N., and Corn, J.E. (2018). CRISPR-Cas9 genome editing in human cells occurs via the Fanconi anemia pathway. *Nat. Genet.* 50, 1132–1139. <https://doi.org/10.1038/s41588-018-0174-0>.
- Feng, Y.C., Liu, X.Y., Teng, L., Ji, Q., Wu, Y., Li, J.M., Gao, W., Zhang, Y.Y., La, T., Tabatabaee, H., et al. (2020). c-Myc inactivation of p53 through the pan-cancer lncRNA MILIP drives cancer pathogenesis. *Nat. Commun.* 11, 4980. <https://doi.org/10.1038/s41467-020-18735-8>.
- Petr, M., Helma, R., Polášková, A., Krejčí, A., Dvořáková, Z., Kejnovská, I., Navrátilová, L., Adámik, M., Vorlíčková, M., and Brázdová, M. (2016). Wild-type p53 binds to MYC promoter G-quadruplex. *Biosci. Rep.* 36, e00397. <https://doi.org/10.1042/BSR20160232>.
- Olivero, C.E., Martínez-Terroba, E., Zimmer, J., Liao, C., Tesfaye, E., Hooshdaran, N., Schofield, J.A., Bendor, J., Fang, D., Simon, M.D., et al. (2020). p53 Activates the Long Noncoding RNA Pvt1b to Inhibit Myc and Suppress Tumorigenesis. *Mol. Cell* 77, 761–774.e8. <https://doi.org/10.1016/j.molcel.2019.12.014>.
- Sachdeva, M., Zhu, S., Wu, F., Wu, H., Walia, V., Kumar, S., Elble, R., Watabe, K., and Mo, Y.Y. (2009). p53 represses c-Myc through induction of the tumor suppressor miR-145. *Proc. Natl. Acad. Sci. USA* 106, 3207–3212. <https://doi.org/10.1073/pnas.0808042106>.
- Morcelle, C., Menoyo, S., Morón-Duran, F.D., Tauler, A., Kozma, S.C., Thomas, G., and Gentilella, A. (2019). Oncogenic MYC Induces the Impaired Ribosome Biogenesis Checkpoint and Stabilizes p53 Independent of Increased Ribosome Content. *Cancer Res.* 79, 4348–4359. <https://doi.org/10.1158/0008-5472.CAN-18-2718>.
- Liao, P., Zeng, S.X., Zhou, X., Chen, T., Zhou, F., Cao, B., Jung, J.H., Del Sal, G., Luo, S., and Lu, H. (2017). Mutant p53 Gains Its Function via c-Myc Activation upon CDK4 Phosphorylation at Serine 249 and Consequent PIN1 Binding. *Mol. Cell* 68, 1134–1146.e6. <https://doi.org/10.1016/j.molcel.2017.11.006>.
- Lindström, M.S., and Wiman, K.G. (2003). Myc and E2F1 induce p53 through p14ARF-independent mechanisms in human fibroblasts. *Oncogene* 22, 4993–5005. <https://doi.org/10.1038/sj.onc.1206659>.
- Cottle, D.L., Kretschmar, K., Schweiger, P.J., Quist, S.R., Gollnick, H.P., Natsuga, K., Aoyagi, S., and Watt, F.M. (2013). c-MYC-induced sebaceous gland differentiation is controlled by an androgen receptor/p53 axis. *Cell Rep.* 3, 427–441. <https://doi.org/10.1016/j.celrep.2013.01.013>.
- Gong, C., Krupka, J.A., Gao, J., Grigoropoulos, N.F., Giotopoulos, G., Asby, R., Screen, M., Usheva, Z., Cucco, F., Barrans, S., et al. (2021). Sequential inverse dysregulation of the RNA helicases DDX3X and DDX3Y facilitates MYC-driven lymphomagenesis. *Mol. Cell* 81, 4059–4075.e11. <https://doi.org/10.1016/j.molcel.2021.07.041>.
- He, T.C., Sparks, A.B., Rago, C., Hermeking, H., Zawel, L., da Costa, L.T., Morin, P.J., Vogelstein, B., and Kinzler, K.W. (1998). Identification of c-MYC as a target of the APC pathway. *Science* 281, 1509–1512. <https://doi.org/10.1126/science.281.5382.1509>.
- Chen, J., Bardes, E.E., Aronow, B.J., and Jegga, A.G. (2009). ToppGene Suite for gene list enrichment analysis and candidate gene prioritization. *Nucleic Acids Res.* 37, W305–W311. <https://doi.org/10.1093/nar/gkp427>.
- Mandal, R., Kohoutova, K., Petrvalska, O., Horvath, M., Srb, P., Veverka, V., Obsilova, V., and Obsil, T. (2022). FOXO4 interacts with p53 TAD and CRD and inhibits its binding to DNA. *Protein Sci.* 31, e4287. <https://doi.org/10.1002/pro.4287>.
- Baar, M.P., Brandt, R.M.C., Putavet, D.A., Klein, J.D.D., Derks, K.W.J., Bourgeois, B.R.M., Stryeck, S., Rijksen, Y., van Willigenburg, H., Feijtel, D.A., et al. (2017). Targeted Apoptosis of Senescent Cells Restores Tissue Homeostasis in Response to Chemotoxicity and Aging. *Cell* 169, 132–147.e16. <https://doi.org/10.1016/j.cell.2017.02.031>.
- Brenkman, A.B., de Keizer, P.L.J., van den Broek, N.J.F., Jochemsen, A.G., and Burgering, B.M.T. (2008). Mdm2 induces mono-ubiquitination of FOXO4. *PLoS One* 3, e2819. <https://doi.org/10.1371/journal.pone.0002819>.
- Oteiza, A., and Mechti, N. (2011). The human T-cell leukemia virus type 1 oncoprotein tax controls forkhead box O4 activity through degradation by the proteasome. *J. Virol.* 85, 6480–6491. <https://doi.org/10.1128/JVI.00036-11>.

26. Brunet, A., Bonni, A., Zigmond, M.J., Lin, M.Z., Juo, P., Hu, L.S., Anderson, M.J., Arden, K.C., Blenis, J., and Greenberg, M.E. (1999). Akt promotes cell survival by phosphorylating and inhibiting a Forkhead transcription factor. *Cell* 96, 857–868. [https://doi.org/10.1016/s0092-8674\(00\)80595-4](https://doi.org/10.1016/s0092-8674(00)80595-4).
27. Hernández-Muñoz, I., Lund, A.H., van der Stoop, P., Boutsma, E., Muijers, I., Verhoeven, E., Nusinow, D.A., Panning, B., Marahrens, Y., and van Lohuizen, M. (2005). Stable X chromosome inactivation involves the PRC1 Polycomb complex and requires histone MACROH2A1 and the CULLIN3/SPOP ubiquitin E3 ligase. *Proc. Natl. Acad. Sci. USA* 102, 7635–7640. <https://doi.org/10.1073/pnas.0408918102>.
28. Chen, D., Zhang, J., Li, M., Rayburn, E.R., Wang, H., and Zhang, R. (2009). RYBP stabilizes p53 by modulating MDM2. *EMBO Rep.* 10, 166–172. <https://doi.org/10.1038/embor.2008.231>.
29. Gonen, N., Futtner, C.R., Wood, S., Garcia-Moreno, S.A., Salamone, I.M., Samson, S.C., Sekido, R., Poulat, F., Maatouk, D.M., and Lovell-Badge, R. (2018). Sex reversal following deletion of a single distal enhancer of Sox9. *Science* 360, 1469–1473. <https://doi.org/10.1126/science.aas9408>.
30. Tang, L., Jin, J., Xu, K., Wang, X., Tang, J., and Guan, X. (2020). SOX9 interacts with FOXC1 to activate MYC and regulate CDK7 inhibitor sensitivity in triple-negative breast cancer. *Oncogenesis* 9, 47. <https://doi.org/10.1038/s41389-020-0232-1>.
31. Hao, Y.H., Lafita-Navarro, M.C., Zacharias, L., Borenstein-Auerbach, N., Kim, M., Barnes, S., Kim, J., Shay, J., DeBerardinis, R.J., and Conacci-Sorrell, M. (2019). Induction of LEF1 by MYC activates the WNT pathway and maintains cell proliferation. *Cell Commun. Signal.* 17, 129. <https://doi.org/10.1186/s12964-019-0444-1>.
32. Jesse, S., Koenig, A., Ellenrieder, V., and Menke, A. (2010). Lef-1 isoforms regulate different target genes and reduce cellular adhesion. *Int. J. Cancer* 126, 1109–1120. <https://doi.org/10.1002/ijc.24802>.
33. Lim, S.K., and Hoffmann, F.M. (2006). Smad4 cooperates with lymphoid enhancer-binding factor 1/T cell-specific factor to increase c-myc expression in the absence of TGF-beta signaling. *Proc. Natl. Acad. Sci. USA* 103, 18580–18585. <https://doi.org/10.1073/pnas.0604773103>.
34. Park, J.W., and Bae, Y.S. (2019). Dephosphorylation of p53 Ser 392 Enhances Trimethylation of Histone H3 Lys 9 via SUV39h1 Stabilization in CK2 Downregulation-Mediated Senescence. *Mol. Cells* 42, 773–782. <https://doi.org/10.14348/molcells.2019.0018>.
35. Zheng, H., Chen, L., Pledger, W.J., Fang, J., and Chen, J. (2014). p53 promotes repair of heterochromatin DNA by regulating JMJD2b and SUV39H1 expression. *Oncogene* 33, 734–744. <https://doi.org/10.1038/ncr.2013.6>.
36. Puschendorf, M., Terranova, R., Boutsma, E., Mao, X., Isono, K.I., Brykczynska, U., Kolb, C., Otte, A.P., Koseki, H., Orkin, S.H., et al. (2008). PRC1 and Suv39h specify parental asymmetry at constitutive heterochromatin in early mouse embryos. *Nat. Genet.* 40, 411–420. <https://doi.org/10.1038/ng.99>.
37. Mädge, B., Geisen, C., Mörry, T., and Schwab, M. (2003). Yaf2 inhibits Myc biological function. *Cancer Lett.* 193, 171–176. [https://doi.org/10.1016/s0304-3835\(02\)00696-1](https://doi.org/10.1016/s0304-3835(02)00696-1).
38. Álvarez, M.M., Biayna, J., and Supek, F. (2022). TP53-dependent toxicity of CRISPR/Cas9 cuts is differential across genomic loci and can confound genetic screening. *Nat. Commun.* 13, 4520. <https://doi.org/10.1038/s41467-022-32285-1>.
39. Sinha, S., Barbosa, K., Cheng, K., Leiserson, M.D.M., Jain, P., Deshpande, A., Wilson, D.M., 3rd, Ryan, B.M., Luo, J., Ronai, Z.A., et al. (2021). A systematic genome-wide mapping of oncogenic mutation selection during CRISPR-Cas9 genome editing. *Nat. Commun.* 12, 6512. <https://doi.org/10.1038/s41467-021-26788-6>.
40. Ritchie, M.E., Phipson, B., Wu, D., Hu, Y., Law, C.W., Shi, W., and Smyth, G.K. (2015). limma powers differential expression analyses for RNA-sequencing and microarray studies. *Nucleic Acids Res.* 43, e47. <https://doi.org/10.1093/nar/gkv007>.
41. Köferle, A., Schlattl, A., Hörmann, A., Thatikonda, V., Popa, A., Spreitzer, F., Ravichandran, M.C., Supper, V., Oberndorfer, S., Puchner, T., et al. (2022). Interrogation of cancer gene dependencies reveals paralog interactions of autosome and sex chromosome-encoded genes. *Cell Rep.* 39, 110636. <https://doi.org/10.1016/j.celrep.2022.110636>.
42. Venkataramanan, S., Gadek, M., Calviello, L., Wilkins, K., and Floor, S.N. (2021). DDX3X and DDX3Y are redundant in protein synthesis. *RNA* 27, 1577–1588. <https://doi.org/10.1261/ma.078926.121>.
43. Navarro-Cobos, M.J., Balaton, B.P., and Brown, C.J. (2020). Genes that escape from X-chromosome inactivation: Potential contributors to Klinefelter syndrome. *Am. J. Med. Genet. C Semin. Med. Genet.* 184, 226–238. <https://doi.org/10.1002/ajmg.c.31800>.
44. Benjamini, Y., and Hochberg, Y. (1995). Controlling the False Discovery Rate: A Practical and Powerful Approach to Multiple Testing. *J. Roy. Stat. Soc. B* 57, 289–300. <https://doi.org/10.1111/j.2517-6161.1995.tb02031.x>.

STAR★METHODS

KEY RESOURCES TABLE

REAGENT or RESOURCE	SOURCE	IDENTIFIER
Deposited data		
CRISPR-Cas9 gene KO effects	DepMap, 22Q4	https://depmap.org
Genes with p53 PPI	STRING database	https://string-db.org
Software and algorithms		
R v3.6.3	R project	https://cran.r-project.org
ggpubr v.0.4.0	N/A	https://rpkgs.datanovia.com/ggpubr
ggplot2 v3.3.0	N/A	https://ggplot2.tidyverse.org
ToppGene	Cincinnati Children's Hospital Medical Center	https://toppgene.cchmc.org/enrichment.jsp
limma v3.42.2	Gordon Smyth	http://bioinf.wehi.edu.au/limma

RESOURCE AVAILABILITY

Lead contact

Further information and requests for resources and reagents should be directed to and will be fulfilled by the lead contact Yuanyan Xiong (xyyan@mail.sysu.edu.cn).

Materials availability

This study did not generate new unique reagents.

Data and code availability

- This paper analyzes existing, publicly available data. These accession numbers for the datasets are listed in the [key resources table](#). All datasets are available within the article or its [supplemental information](#). DepMap data were downloaded from <https://depmap.org/>. Protein-protein interactions with *TP53* were downloaded from STRING (<http://string-db.org/>).
- This paper does not report original code. Any additional information required to reanalyze the data reported in this paper is available from the [lead contact](#) upon reasonable request.

METHOD DETAILS

Data collection, preprocessing, and summary

We obtained processed data of gene editing KO effects for CRISPR screening, gene mutations from Cancer Cell Line Encyclopedia (CCLE), and all cell line information from the DepMap project (22Q4, <https://depmap.org/portal/>). CRISPR KO effects were defined by the depletion of guide RNAs (gRNA) after CRISPR-Cas9 introduction into cell lines followed by sequencing and were calculated by comparing gRNA numbers in the initial cells at the beginning with those in the cells cultured for a period of time. Cell lines (excluded if with 'unknown' sex information) were separated into two groups by p53 status, p53-WT and p53-MUT (with p53 non-silent mutations as defined in the Enache et al. study). For both p53 groups, cell lineages with ≥ 10 samples (at least 3 samples for both males and females) were retained for downstream analysis. First, we tested the sex-biased KO effects in each cell lineage for a list of 2,007 genes (termed 'gene set 1') encoding proteins interacting with p53, obtained from the PPI database STRING (<https://string-db.org/>) by requiring interaction confidence scores larger than 400. Then, we extended the test to all genes ($n = 17,454$, termed 'gene set 2') screened by DepMap. Differential KO effects between sexes for each tissue were compared by two-sided t-test. Cross-tissue sex-biased KO effects were obtained by applying limma⁴⁰ to KO effects of all cell lines (excluding those from sex-specific tissues: breast, cervix, ovary, prostate, uterus) at the same time, with sex and tissue type as covariables.

Of note, seven genes (EDA2R, MYC, PIK3CA, PPEF1, PSMC4, SUV39H1, and TLR7) were identified as significant based on both 'gene set 1' and 'gene set 2', and only annotated as genes whose protein products with p53 PPI. Moreover, five genes (DDX3X, EIF1AX, RPS4X, ZFX, MAGEH1, and VBP1) showed significant CRISPR-Cas9 sex bias in both p53-WT and p53-MUT samples and were excluded. Among them, DDX3X, EIF1AX, and ZFX are functionally linked with their paralogs encoded by the Y chromosome in males (DDX3Y, EIF1AY, and ZFY, respectively)^{41,42} and escape X inactivation in females.⁴³ The potential loss of chromosome Y in some male samples or reactivation of chromosome X in some female samples may explain these results.

Number of cell lines for each tissue used in the CRISPR-Cas9 analysis were as following: bile_duct (n = 20), blood (n = 49), bone (n = 25), central_nervous_system (n = 66), colorectal (n = 46), esophagus (n = 30), eye (n = 7), gastric (n = 27), kidney (n = 20), liver (n = 22), lung (n = 125), lymphocyte (n = 34), pancreas (n = 41), peripheral_nervous_system (n = 24), plasma_cell (n = 18), skin (n = 52), soft_tissue (n = 27), thyroid (n = 13), upper_aerodigestive (n = 51), urinary_tract (n = 28). The subgroup numbers regarding to p53 status (WT or MUT) and sex (male or female) were shown in [Table S2](#).

Enrichment analysis

Functional enrichment analysis of significant genes with sex bias of CRISPR-Cas9 editing (PCSB genes) was performed by using the web server of ToppGene (<https://toppgene.cchmc.org/enrichment.jsp>), which used 26,918 and 20,915 genes as the background for enrichment of "transcription factor binding sites" and "cellular component", respectively, by default.²¹

QUANTIFICATION AND STATISTICAL ANALYSIS

Throughout this study, p-values were corrected for multiple testing by the Benjamini & Hochberg (or false discovery rate, FDR) correction⁴⁴ by using the R function `p.adjust`. Adjusted p-values smaller than 0.2 were considered significant and raw p-values less than 2e-3 were considered suggestive. All analysis and visualizations were performed using R language (<http://www.r-project.org/>). Data are presented as median \pm interquartile range (IQR). The level of significance was indicated by the p value. Bootstrapping was used to assess significance of the sex-bias of Cas9 activity differences between MUT and WT p53 cell lines. A total of 100 random samples were obtained from Cas9 activities of cell lines, and Cas9 differences for each sex between MUT and WT p53 were calculated for each random sample.